ChemPubSoc Europe

DOI: 10.1002/slct.201700726

Chemistry SELECT Full Papers

Electro, Physical & Theoretical Chemistry

Molecular Insights into Protein-Polyphenols Aggregation: A Dynamic and Topological Description

André N. Petelski,[a, b] Silvana C. Pamies,[a] Elisa I. Benítez,[a, b] María M. Lataza Rovaletti,[a] and Gladis L. Sosa*[a, b]

Protein-polyphenols interactions are of greatest interest in several fields like food technology and leather industry. Also, it is thought that these interactions are responsible for the undesired phenomenon of colloidal turbidity. However, there is sparse information about the molecular implications leading to this phenomenon. In this study, Molecular Dynamic (MD) simulations in conjunction with the analysis of the topology of the electron density are used to study protein/polyphenol interactions in a model system which consists of a ternary mixture of water, the flavonoids Catechin and Procianidin B3 and proline pentapeptides. After 50 ns of simulation, root mean square deviation, root mean square fluctuation and number of hydrogen bonds were calculated. Information about the intermolecular interactions that drive the assembly of colloidal complexes has been obtained by the analysis of the electron charge density. Results show the formation of a stable adduct, with a very complex network of conventional and non-conventional hydrogen bonds. This study has also shown the significance of C-H···O and C-H···π interactions in the phenomenon of colloidal turbidity.

1. Introduction

During the last years, interactions between proteins and polyphenols have been subject of several researches due to their biological effects.[1–3] Most of these works aim to clarify both, the bonding mechanisms and the conditions under which they are produced.

In production of fruit juices and fermented beverages like beer, many investigations using experimental techniques have demonstrated that these interactions are mainly responsible for the undesirable phenomenon of colloidal turbidity, in which proline-rich polypeptides and polyphenols combine to produce a visible haze that causes unpleasant organoleptic sensations and reduces the lifetime of beverages.[4,5] It has been suggested that the bonding mechanism is non-covalent, in which proteins are held together through polyphenolic compounds that act as bridges,[6,7]the binding is produced through hydrogen bonds (HBs) in sites where mainly proline **1** (Pro) residues are presents. In addition, Oh et al. have concluded that hydrophobic bonding are dominant in protein-polyphenol complexes.[8]Asano and co-workers have shown that peptides with a higher molar percentage of Pro tend to form more haze (turbidity), while synthetic polypeptides lacking of that amino acid do not form haze;[9] in their model, a linear relationship between the molar percentage of Pro and the haze formation at a constant concentration of Catechin **2** has been verified. In other model systems, with different proteins and polyphenolic compounds, it has also been verified that poly-hidroxyproline do not produce haze at any concentration, gelatin produces a peak of haze at low concentrations with tannic acid and practically no haze with Catechin, while Gliadin (a class of protein present in wheat) produces more haze with tannic acid than other polypeptides.[7] The amount of haze formed is a function of protein and polyphenols concentrations, and the relationship between them.

In leather industry, interactions between tannins (a polyphenols mixture) and skin collagen (a Pro rich protein) have been to date the basis of tanning techniques, by which animal skin has been turned into leather since immemorial times.[10,11]

On the one hand, in disciplines related to health, it has been pointed out that the binding of polyphenols to enzymatic proteins can induce denaturalization and loss of catalytic activity.[12–15] It is believed that the binding established has a hydrophobic nature resulting in the formation of aggregates or insoluble complexes that finally precipitate.[16,17] By using docking and molecular dynamic (MD) simulations it has been shown that the binding to the active site is established by short HBs and Van der Walls interactions, resulting in the formation of protein-polyphenol complexes.[18,19] Xuli Wu and co-workers have indicated the loss of catalytic activity in Lipase by (-)-Epigallocatechin-3-gallate (EGCG) from Green tea,[20] pointing out that in a first step the interactions are hydrophobic and then the complex is stabilized by HBs. These interactions alter the conformational structure of the protein that may results in a decrease of catalytic activity.

[a] A. N. Petelski, S. C. Pamies, Dr. E. I. Benítez, M. M. L. Rovaletti, Dr. G. L. Sosa
Chemical Engineering Department.
Grupo de Investigación en Química Teórica y Experimental (QuiTEx), Facultad Regional Resistencia, Universidad Tecnológica Nacional,
French 414 (H3500CHJ), Resistencia, Chaco, Argentina
E-mail: glsosa@frre.utn.edu.ar

[b] A. N. Petelski, Dr. E. I. Benítez, Dr. G. L. Sosa
Instituto de Química Básica y Aplicada del Nordeste Argentino (IQUIBA-NEA), UNNE-CONICET.
Avenida Libertad 5460 (3400), Corrientes, Argentina.

Supporting information for this article is available on the WWW under https://doi.org/10.1002/slct.201700726

On the other hand, flavonoids present in beverages like wine and tea interact with proteins from saliva secreted in the oral cavity, which results in the phenomenon known as astringency.[21,22] Salivary Pro rich proteins form insoluble complexes with polyphenols that then precipitate, thus reducing the lubricant properties of saliva,[23] which is felt in a dry puckering-like sensation. In experimental researches with a synthetic salivary Pro-rich peptide and different polyphenols, Baxter and co-workers have concluded that the main forces are of hydrophobic character, although HBs play a secondary roll.[24] To date, several researches have argued that polyphenols bind preferably to Pro amino acids, in different models of proteins, by means of MD and Docking techniques combined with experimental techniques. In model complexes formed by procyanidin B3 **3** (PB3) and the human salivary protein fragment IB7 (aminoacid sequence: SPPGKPQGPPPQGG), Simon et al.[25] have suggested that the binding of the polyphenol to the protein reduces their conformational disorder, the complex is stabilized by HBs between carbonyl groups of Pro residues and OH groups of procyanidin, although they have pointed out that the H-bonding pattern is rather complicated. In a model complex between EGCG and a model Pro-rich peptide, in line with other hydrophobic interactions mentioned, Charlton et al.[26] have shown that the main interaction is a face to face stacking interaction, between the EGCG ring and Pro ring, with a hydrophobic character, with some possible interactions with Arginine. A similar model has been studied by Canon et al.[27] based on IB5 salivary protein and EGCG, in which they have shown evidences of structural changes in the protein after a complex formation; initially, the protein adopts an open conformation (due to Pro residues) then, it binds to at least 5 polyphenols resulting in a more compacted structure. Very recently, Ferrer-Gallego et al.[28] have concluded the same using similar systems.

To our knowledge, and until now, the nature of the interactions has been described as hydrophobic interactions or contacts that involve stacking interactions between aromatic rings of polyphenols and Pro residues.[29] Also, it has been suggested that polyphenols bind to proteins by HBs of O-H···O type between carbonyl groups of Pro preferably and -OH groups of plolyphenols. However, hydrophobic interactions have not been fully described yet, remaining many issues related to these interactions still unresolved.

The aim of this study is to contribute to the understanding of the mechanism by which polyphenols bind to proteins and perform a deeper insight upon the molecular interactions that conduct to complex formation. For this purpose we studied, with different theoretical tools, model systems formed by pentapeptides of Pro **1** (PP) and two polyphenol compounds, (+)-Catechin **2** (CAT) and procyanidin B3 **3** (see Figure 1) embedded in an aqueous environment. Techniques of MD simulations were used to study the complexation mechanism. The interactions involved in the resulting complexes were studied by the Quantum Theory of Atoms in Molecules (QTAIM) of Bader[30] after optimizing structures at the semiempirical PM6 method.

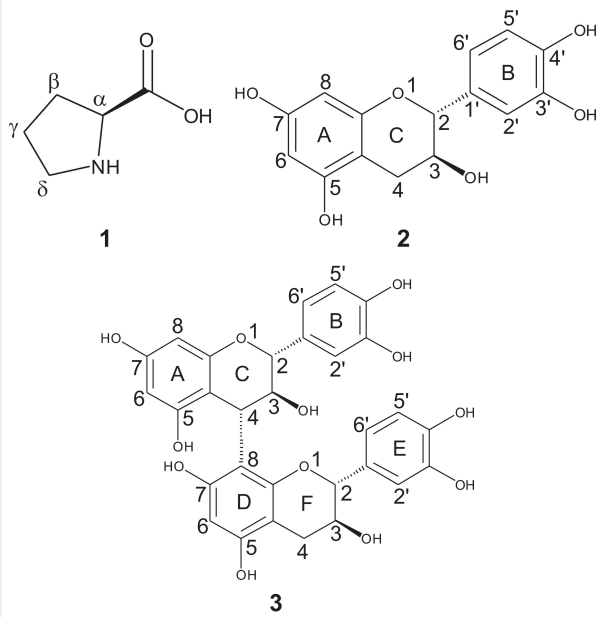

Figure 1. Molecular structures of proline **1**, (+)-catechin **2**, and procyanidin B3 **3.**

2. Results and Discussion

2.1. PP-CAT system

Hydration of the protein

The structure and dynamics of solvent molecules was evaluated through the Radial Distribution Function (RDF) which calculates the probability of finding a pair of atoms at a distance *r*, compared to an expected probability for a random distribution to the same density. This statistic tool allows examining the interactions water-water and water-solute that describe the hydration of solutes. In several simulations,[31,32] the RDF has been used to detail the differences between the first and the second hydration layer of different solute atoms. This is particularly useful to show both, the hydrophobic behavior of carbon atoms and hydrophilic behavior of oxygen atoms.[33]

In order to examine the preferred hydration sites on the peptide and the water-solute interactions involved in the system, the $g_{ij}(r)$ solute-solvent RDFs were calculated for the solvent atom j (water oxygen atoms) around the i solute atoms (either the, Pro oxygen or Pro carbon atoms), and they are shown in Figure 2. In Figure 2a it is observed that four O atoms of the backbone are hydrated showing a pick at a distance of 2.8 Å. This is referred as the first hydration shell and since a defined second peak is not observed the interactions are not enough to maintain a second hydration layer. The fact that O_2 of Pro residue ($O_{2\text{-Pro}}$) does not display a peak (red line of Fig. 2a) shows that it is disabled to the access of water, as it will be discussed later.

In Figure 2b it is evidenced the low occurrence probability of water oxygen atoms around C atoms, which indicates a poor hydration. The Cγ, which is the furthest away from the

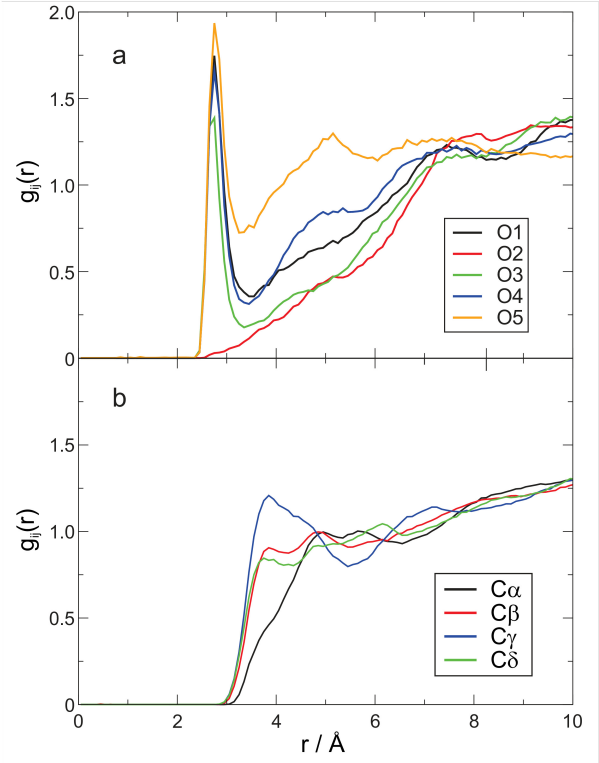

Figure 2. Radial distribution function of **(a)** water oxygen atoms around proline oxygen atoms of each residues, and **(b)** water oxygen atoms around proline carbon atoms; calculated for the last 5 ns.

backbone, shows a broad pick at approximately 3.8 Å, which indicates a little hydration shell.

Intermolecular hydrogen bonds

VMD analysis surprisingly shows that, despite the great number of -OH groups of CAT, just one interaction between CAT and the PP is revealed. An interaction is broken and formed continuously at the beginning of the simulation until reaching an evident stability after 20 ns of production. At this point a second HB appears but intermittently. The analysis of occupancy and lifetimes during the last nanosecond reveals again just one HB: $O_{3'B}$–H···$O_{2\text{-}Pro}$, with an occupancy percentage of 70.9% and a lifetime of 16.9 ps. These values suggest that this interaction is relatively stable. With regards to the second HB, it occurs between CAT –O_{7A}–H group and C=O group of Pro-3 residue. In addition, it was found that both oxygen atoms, O_{7A} and $O_{3\text{-}Pro}$, are involved in an inter-residue water bridge, in which a water molecule is positioned between these O atoms by disrupting the O_{7A}–H···$O_{3\text{-}Pro}$ HB. That is, a water molecule connects both O atoms through two HBs: O_{7A}–H···O_W–H···$O_{3\text{-}Pro}$=C (see Figure 3). This water molecule is exchanged rapidly with the bulk solvent and since the O_{7A}–H···$O_{3\text{-}Pro}$ interaction is disrupted several times by this interchange; thus, it shows very low percentages of occupancy and lifetime. However, this fact reflects how the solvent cooperates with the stabilization of the complex.

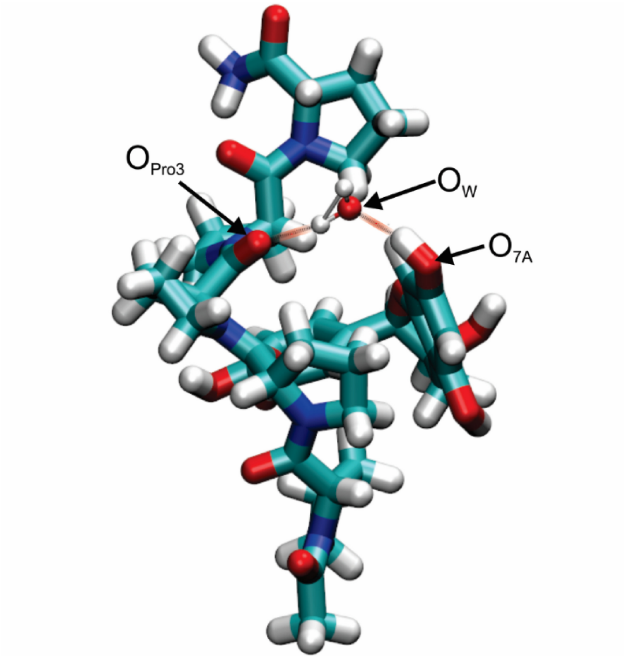

Figure 3. Snapshot of CAT-PP complex showing how the water molecule disrupt the O_{7A}-H···$O_{3\text{-}Pro}$ HB (O_{7A}-H···Ow-H···$O_{3\text{-}Pro}$). The water molecule (TIP3P model) is represented with ball and sticks.

The intermolecular HBs analysis between the peptide and water molecules is shown in Figure 4. The low occupancy

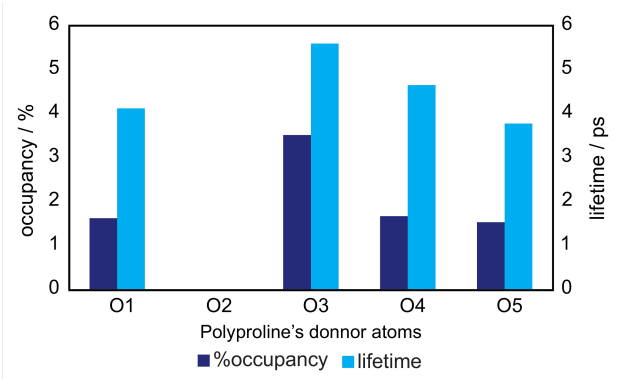

Figure 4. Average lifetimes and % of occupancy of O-H···O HBs for each pentapeptide O atom.

percentages can be seen if they are compared with the HB analysis between the CAT and the PP. In line with RDF results, it is observed that the O_2 of Pro does not participate in any interaction with water because it is involved in the $O_{3'B}$–H···$O_{2\text{-}Pro}$ HB.

In order to analyze the consistency of HBs between CAT and PP, the $O_{3'B}$···$O_{2\text{-}Pro}$ interatomic distance as a function of the simulation time was calculated. The plot (see Figure 5) clearly shows that after 20 ns of big fluctuations, the formation of the

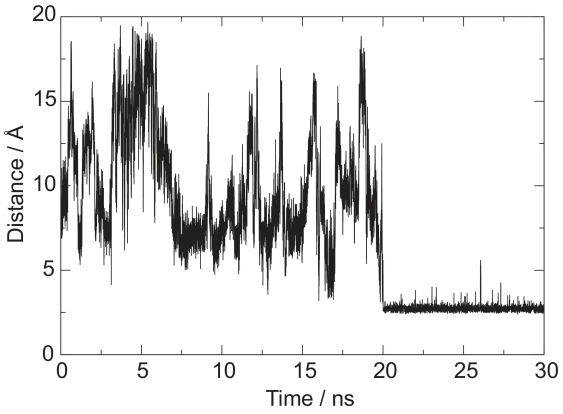

Figure 5. Interatomic distance between $O_{3'}$ of Catechin and O_2 of Proline residue (distance corresponded to the HB $O_{3'C}$-H···$O_{2\text{-Pro}}$) as a function of the simulation time.

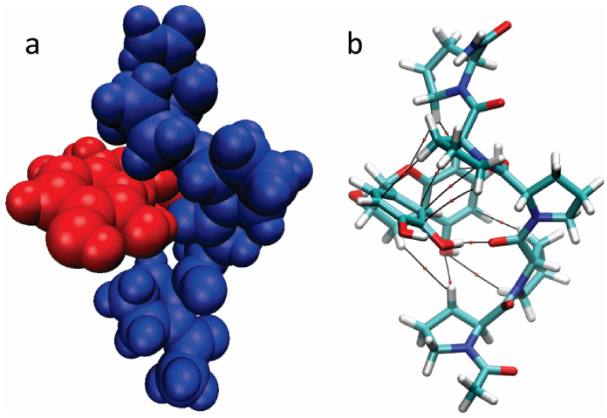

Figure 6. (a) Snapshot of the lowest potential energy structure, obtained from the MD step production. **(b)** Molecular Graph showing the intermolecular interactions, LCPs are colored in red.

HB with an average distance of approximately 2.69 Å is verified, in good agreement with a distance of a typical HB. This distance remains practically constant after 10 ns of the MD with a very low fluctuation, being a clear evidence of the complex formation mediated by HB interactions. The analysis of the occupancy percentage during these 10 ns was calculated in 77.5% with a lifetime of 22.9 ps.

Finally, a more rigorous analysis of intermolecular interactions was performed with the QTAIM method.[30] This methodology has been successfully applied in the study of the properties of a variety of conventional and non-conventional HBs, and $\pi-\pi$ stacking interactions,[34,35] and currently it is used universally as a test for the existence of bonding interactions.[36] In the QTAIM context, a bond between two atoms is described by a line of maximum electron density, the bond path, which connects the respective nuclei and intersects the zero-flux surface of the electron density gradient field ($\nabla\rho(r_c)$) at the so called bond critical point (BCP). However, a new terminology was recently proposed: line critical point[37,38] (LCP), which is adopted herein. In this work, different topological properties evaluated at the LCPs were used to characterize the interactions: the electron charge density, $\rho(r_c)$, which measures the accumulation of charge between the bonded nuclei and reflects the bond strength;[39–42] the Laplacian of the electron density $\nabla^2\rho(r_c)$, that reveals the local charge concentration ($\nabla^2\rho(r_c) < 0$) or depletion ($\nabla^2\rho(r_c) > 0$); the ellipticity ε at the LCP, that shows structural and topological instability[38,43]; and the index $|V(r_c)|/G(r_c)$, that quantifies the strength of an HB within three regions[44,45]: an HB interaction is defined as a weak when $|V(r_c)|/G(r_c) < 1$, as closed-shared with some covalent character when the ratio falls between 1 and 2, and as strong HBs and covalent bonds when $|V(r_c)|/G(r_c) > 2$.[45] A minimum potential energy structure was extracted from the production simulations without considering all water molecules, which is shown in Figure 6a. This complex occurs at 23.35 ns of the simulation in line with the stable distance from Figure 5. The structure was subjected to a semiempirical optimization and then a wave function was generated at the ω-B97XD/6-311++G** level of theory. The results of the QTAIM analysis are shown in Table 1 and the molecular graph of the CAT/PP complex is displayed in Figure 6b, in which the LCPs corresponding to the covalent bonds were omitted in order to emphasize just the intermolecular interactions.

Table 1. Local properties at molecular interaction LCPs within a selected complex.

Interaction	$\rho(\mathbf{r}_c)$	$\nabla^2\rho(\mathbf{r}_c)$	$\lvert V(\mathbf{r}_c)\rvert/G(\mathbf{r}_c)$	ε
$H_{\beta1}$···H_{4C}	0.0010	0.0041	0.5981	0.2054
$C_{\delta2}$-H···O_{5A}	0.0018	0.0067	0.6907	0.4303
$C_{\delta4}$-H···$C_{3'B}$	0.0023	0.0080	0.7304	0.6594
N_2···$C_{2'B}$	0.0030	0.0086	0.8207	0.3989
$C_{\beta1}$-H···O_{5A}	0.0032	0.0118	0.7579	0.0455
$C_{\alpha4}$-H···$C_{2'B}$	0.0034	0.0106	0.7740	0.5088
C=$O_{3\text{-Pro}}$···C_{8A}	0.0048	0.0151	0.7970	0.3845
$H_{\delta5}$···H_{8A}	0.0053	0.0156	0.8108	0.1609
$C_{\beta2}$-H···O_{6A}	0.0055	0.0152	0.7916	0.4313
$C_{\delta5}$-H···O_{1C}	0.0056	0.0180	0.8431	0.0167
$C_{\beta4}$-H···$C_{5'B}$	0.0068	0.0200	0.8162	2.4618
$O_{3'B}$-H···$O_{2\text{-Pro}}$	0.0277	0.1137	0.9011	0.0452

All values are in atomic units.

The QTAIM analysis reveals the existence of several closed shell interactions. From Table 1 it can be seen just one strong HB in which the $O_{3'B}$ of CAT is acting as a proton donor, and the C=O group of the Pro 2 residue acts as the proton-acceptor counterpart, as was previously observed in the MD results. The Laplacian is positive and the value falls within the proposed rang of 0.014 - 0.139 au.[43] Thus, the $O_{3'B}$-H···$O_{2\text{-Pro}}$ interaction corresponds to a weak HB. In addition, the stability of this HB is also reflected in its low value of ellipticity. Furthermore, non-conventional HBs of the C–H···O type between C atoms of Pro rings and -OH groups of CAT are revealed, that is: $C_{\delta2}$-H···O_{5A}, $C_{\beta1}$–H···O_{5A}, $C_{\beta2}$–H···O_{6A}, $C_{\delta5}$–H···O_{1C}. The density values at these LCPs were found to vary from 0.001 to 0.006 au, in agreement with values reported by other authors[46,47] in which this

quantity was found to vary from 0.002 to 0.034 au. As can be seen in Table 1, the $|V(r_c)|/G(r_c)$ and ε values obtained for the $C_{\delta5}$–H···O_{1C} and $C_{\beta1}$–H···O_{5A} interactions would indicate that these HBs are stronger than $C_{\delta2}$-H···O_{5A}, and $C_{\beta2}$–H···O_{6A} HBs.

As it was previously mentioned, Oh et al.[8] and also Ferrer-Gallego et al.[28] have claimed that protein-polyphenol interactions are mainly due to hydrophobic contacts. This interaction was also described as a stacking interaction between a polyphenolic aromatic ring and a proline pyrrolidone ring.[29] This fact is observed here as non-covalent interactions of C–H···π type: $C_{\delta4}$–H···$C_{3'B}$, $C_{\alpha4}$–H···$C_{2'B}$, and $C_{\beta4}$–H···$C_{5'B}$, which occur between the B ring of the polyphenol and a Pro ring, leading to a face to face stacking interaction. All values of charge density at LCPs lay in the order of those reported in literature.[48,49] It could be pointed out that the $C_{\beta4}$-H···$C_{5'B}$ HB is the weakest, since it has the greatest value of ellipticity among all the interactions.

Moreover, the so called dihydrogen bonds, H···H, are observed. They occur between H atoms of Pro ring and H atoms of CAT attached to C atoms, i. e., $H_{\delta5}$···H_{8A}, $H_{\beta1}$···H_{4C}. These interactions have been widely studied in the literature by theoretical and experimental methods,[43,50] and they were also observed in other biological systems.[49] The density values of $\rho(r_c)$ at LCPs (which range from 0.001 to 0.005 au) lay in the order of the QTAIM criteria to characterize HBs.[46] However, the $H_{\beta1}$···H_{4C} contact does not fulfill the Laplacian criteria.

Finally, a non-covalent $O_{3\text{-}Pro}$···C_{8A} interaction was revealed. This type of interaction was also found in π-dimers of catechol and quinhydrone[35,48] with density values of $\rho(r_c)$ that vary from 0.004 to 0.006 au. It is also worth highlighting that Mosquera et al. have found that this interaction is more stabilizing than the C–H···π HB in catechol dimers.[48] Therefore, these findings give some relevance to the $O_{3\text{-}Pro}$···C_{8A} LCP.

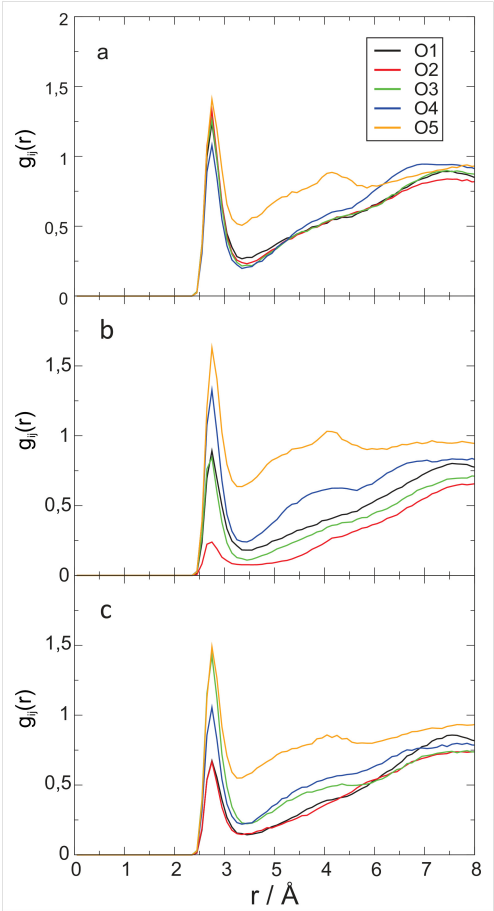

Figure 7. Radial distribution function of water oxygen atoms around oxygen atoms of **(a)** PP 1, **(b)** PP 2 and **(c)** PP 3.

2.2. PP-PB3 System

Hydration of pentapeptides

The RDFs calculated for each PP molecule are displayed in Figures 7 a-c. When looking at the height of the picks, it can be seen from these figures the different behaviors of PP oxygen atoms which are the same for the previous system. Some oxygen atoms are more surrounded by water molecules than others. In fragment 2 and 3 the O_2atoms are strongly disabled to the access of water, probably because they are interacting with polyphenols as it has been demonstrated in the previous system. A second peak corresponding to a second hydration layer is not observed.

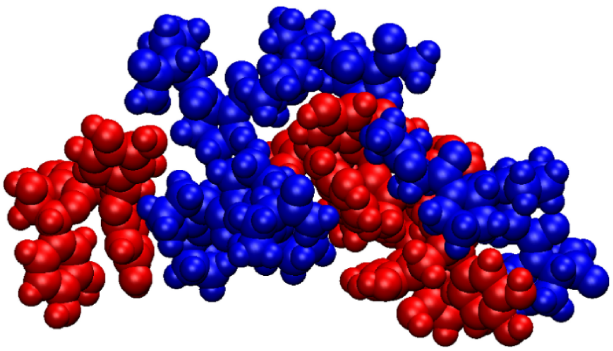

Figure 8. Snapshot of the final structure of complexes. The PB3 molecules are colored at red, and the PP molecules are colored at blue.

Hydrogen bonds

Figure 8 shows a snapshot of the PP-PB3 system, in which a great agglomeration between PP and PB3 molecules is observed. Also, it can be pointed out that PPs are probably interacting with more than one PB3 molecule.

With the collected trajectories from the production step the temporal evolution of the number of HB was calculated, and then the lifetimes and occupancy percentages were evaluated as it has been mentioned above. The analysis shows that the number of HBs range from 1 to 6, a small number if the number of OH groups of the polyphenols and the number of proton acceptors of pentapeptides is considered. However, as it was pointed out in the CAT-PP system, one HB is sufficient for the stabilization of the complex. By analyzing water/peptide

and peptide/polyphenol interactions, the mean occupancy percentages of PP-PB3 HBs are higher than the PP-WAT %, which are practically null. This analysis reveals the greater affinity of the proteins to polyphenols than to water, and it is clear that PB3 molecules are bonded to specific oxygen atoms, which will be discussed in the section hereafter.

Table 2 reports the results of the HB analysis between PP and PB3 molecules: occupancy percentages, lifetimes, and the

Table 2. Hydrogen bond analysis

Interaction	Occupancy %	Lifetime [ps]	Distance [Å]	Angle [°]
$O_{4'B}$–H···$O_{1\text{-}Pro}$	54.90	13.1	2.72	18.27
O_{5A}–H···$O_{1\text{-}Pro}$	92.10	16.2	2.72	19.29
O_{3F}–H···$O_{2\text{-}Pro}$	92.50	17.1	2.73	17.22
O_{7A}–H···$O_{4\text{-}Pro}$	12.40	3.9	2.77	15.75

average values of distances and angles. Taking into account this table, it can be pointed out that the cluster of Figure 8 is held together only by four HBs; therefore, what is generally called "hydrophobic interactions/contacts" gain a special value.

In order to analyze the most stable interaction, by taking into account the higher occupancy and lifetime values of Table 2, the interatomic distance O_{3F}···$O_{2\text{-}Pro}$ as a function of the simulation time was calculated. The results (see Figure 9) show

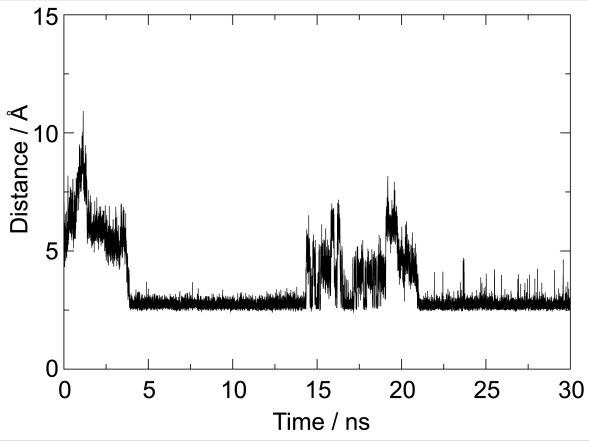

Figure 9. Interatomic distance between O_{5A} of PB3 and O_1 of Proline residue (distance corresponded to the HB O_{5A}–H···$O_{1\text{-}Pro}$) as a function of the simulation time.

again the stability of the complex. The PP and PB3 molecules are bonded by a HB at 4 ns of the simulation, and then the HB breaks to be formed again at 21 ns. Almost the same behavior is observed in the $O_{4'B}$–H···$O_{1\text{-}Pro}$, O_{5A}–H···$O_{1\text{-}Pro}$ and O_{7A}–H···$O_{4\text{-}Pro}$ interactions.

In the same way as in the PP-CAT system, the interactions involved in the complex were analyzed by the QTAIM method. For this purpose a dimer of PP/PB3 was randomly extracted from the production runs and all water molecules were removed. With this structure a wave function was generated at the ω-B97XD/6-311++G** level of theory. The results of the QTAIM analysis are shown in Table 3. In general, all LCPs fulfill

Table 3. Local properties at molecular interaction LCPs within a selected complex.

Interaction	ρ(rc)	∇2ρ(rc)	|V(rc)|/G(rc)	ε
$C_{\beta1}$H···O_{3F}	0.0015	0.0068	0.6515	0.3075
$H_{\gamma2}$···H_{3F}	0.0021	0.0078	0.7286	0.0549
$H_{\beta2}$···H_{3F}	0.0022	0.0077	0.7385	0.1086
$H_{\beta4'}$···$H_{2'B}$	0.0031	0.0100	0.7693	0.9799
C_{2F}-H···$O_{3\text{-}Pro}$	0.0038	0.0126	0.8101	0.0395
$C_{\gamma5}$-H···$O_{4'E}$	0.0042	0.0161	0.8040	1.8403
$C_{\beta5}$-H···$O_{3'E}$	0.0047	0.0159	0.8353	0.1809
$H_{\delta4'}$···$H_{2'B}$	0.0052	0.0148	0.8403	0.2195
$H_{\beta4'}$···H_{8A}	0.0053	0.0183	0.7320	0.8904
$H_{\alpha4'}$···H_{2F}	0.0055	0.0164	0.8286	0.2113
$C_{\delta5}$-H···C_{8A}	0.0059	0.0155	0.8362	0.3403
$C_{\beta1}$-H···$O_{4'E}$	0.0063	0.0211	0.8303	0.5788
$C_{\beta2}$-H···O_{1C}	0.0073	0.0223	0.8728	0.0208
$H_{\delta2}$···$H_{3'B}$	0.0079	0.0236	0.8296	0.0473
$C_{\delta5}$-H···O_{3F}	0.0079	0.0231	0.8907	0.0412
$C_{\delta5}$-H···$C_{3'E}$	0.0085	0.0266	0.8233	2.9924
$C_{2'E}$-H···$O_{3\text{-}Pro}$	0.0096	0.0324	0.8213	0.0613
O_{3F}-H···$O_{2\text{-}Pro}$	0.0291	0.1151	0.9211	0.0537

All values are in atomic units.

the $\rho(r_c)$ and $\nabla^2\rho(r_c)$ criteria for HBs, except the first five interactions of Table 3. The topology analysis reveals, again, the presence of just one HB O–H···O type which is the strongest according to $\rho(r_c)$ and $|V(r_c)|/G(r_c)$ values (see Table 3), as well as the system PP-CAT. Besides, other less usual interactions such as C–H···O, C–H···π and H···H have been detected, similarly to the CAT-PP system. Among these interactions, $C_{\gamma5}$-H···$O_{4'E}$ and $C_{\delta5}$-H···$C_{3'E}$ seem to be the most topologically instable due to their higher ellipticity values. Hence, the binding mechanism of PB3 is essentially equal to that of CAT.

Finally, it has been suggested[51] that polyphenols can act as bridges by linking two chains of proteins at the same time, and this is the presumed mechanism by which the molecular aggregates increase in size to reach the size of the colloid. In order to examine this hypothetical mechanism, we analyzed the interactions by the QTAIM method using the same strategy that was used in the previous systems. A structure was taken from the MD simulation, which includes four molecules, two PP and two PB3 molecules. After a semi-empirical optimization at the PM6 level, the wave function was generated at the HF/6-31G* level of theory. The molecular graph of the complex is shown in Figure 10. This information is essentially qualitative.

In Figure 10< a xfigr10> it can be clearly seen how the PB3 molecule (colored in orange) takes place between two fragments of PP and forms several interactions with both fragments. Also, a stacking interaction between the polyphenolic ring and the Pro ring is observed. As it has been previously mentioned, the stacking interaction is a set of HBs of the C–H···π type, in which C atoms of the polyphenolic ring act as electron donors whereas the C–H bonds of Pro ring act as proton donors (electron acceptors). In addition, interactions of

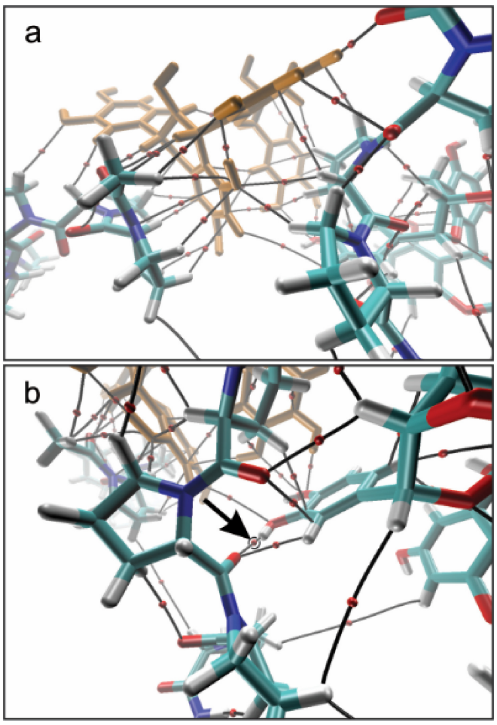

Figure 10. Molecular graph of two PB3 molecules interacting with two PP. **(a)** A PB3 molecule, which is colored in orange, is placed between two peptide chains. **(b)** Molecular graph indicating the $O_{3'B}$–H···O_{Pro} HB. Small red circles correspond to LCP or (3, −1) critical points of intermolecular interactions. Those LCPs corresponding to covalent bonds were omitted for visual clarity.

the C–H···O type are observed, in which C atoms of the protein act as proton donors.

In Figure 10< b xfigr10> it can again be observed a HB of the O–H···O type between the -OH group of the catechol ring and the O atom of the peptidic bond, in conjunction with a second HB C–H···O type. This interaction has a key role in the mechanism of formation of the complex since it occurs in all the structures analyzed in this work, and it shows the greatest value of $\rho(\mathbf{r}_c)$ at the LCP, as it was previously seen. Moreover, polyphenols access to the active site of proteins through this interaction, that is, the carbonylic oxygens.

Conclusions

The theoretical results presented here provide a fundamental description of the molecular interactions involved in protein-polyphenol complexes by combining Molecular Dynamics simulations and electronic structures calculations.

MD results show the formation of stable complexes in time. In the first system, the CAT and PP molecules remain attached during the last 5 ns of simulation whereas in the second one, a stable conglomerate is formed. The topology analysis reveals that the mechanism of interaction relies upon a wide network of HBs involving: O–H···O type and a vast number of non-conventional HBs: C–H···O and C–H···π. In addition, other less usual interactions have been found: O···O, H···H and O···C. The manifestation of these interactions along the peptide chain leads to the formation of polyphenol/protein complexes. Thus, since polyphenols can link at least two peptide chains at the same time, the complexes grow in size until they reach the size of the colloidal particles.

Finally, it can be concluded that the necessary condition for the development of the colloid is the formation of an HB that involves a carbonylic oxygen of the protein and an –OH group of the polyphenol.

Supporting Information Summary

This summary contains details of the computational method followed.

Acknowledgements

We acknowledge SECyT-UTN-FRRe (Secretaría de Ciencia y Tecnología, Universidad Tecnológica Nacional, Facultad Regional Resistencia) for financial support. The AMBER 11 software was donated by AMBER developers. A.N.P. thanks CONICET (Consejo Nacional de Investigaciones Científicas y Técnicas), Argentina, for a doctoral fellowship. E.I.B. is a CONICET career researcher.

Conflict of Interest

The authors declare no conflict of interest.

Keywords: Aggregation · Computational Chemistry · Hydrogen Bonds · Molecular Dynamics · QTAIM

[1] C. G. Fraga, M. Galleano, S. V Verstraeten, P. I. Oteiza, *Mol. Aspects Med.* **2010**, *31*, 435–45.
[2] E. Steiner, T. Becker, M. Gastl, J. I. Brew, *J. Inst. Brew.* **2010**, *116*, 360–368.
[3] G. R. Scollary, G. Pásti, M. Kállay, J. Blackman, A. C. Clark, *Trends Food Sci. Technol.* **2012**, *27*, 25–36.
[4] K. J. Siebert, *LWT - Food Sci. Technol.* **2006**, *39*, 987–994.
[5] S. Tajchakavit, J. I. Boye, D. Bélanger, R. Couture, *Food Res. Int.* **2001**, *34*, 431–440.
[6] L. Chapon, *Brauwelt* **1968**, *108*, 1769–1775.
[7] K. J. Siebert, N. V Troukhanova, P. Y. Lynn, *J. Agric. Food Chem.* **1996**, *44*, 80–85.
[8] H. I. Oh, J. E. Hoff, G. S. Armstrong, L. A. Haff, *J. Agric. Food Chem.* **1980**, *28*, 394–398.
[9] K. Asano, K. Shinagawa, N. Hashimoto, *J. Am. Soc. Brew. Chem.* **1982**, *40*, 147–154.
[10] R. Sutherland, *Ind. Eng. Chem.* **1947**, *39*, 628–631.
[11] G. D. McLaughlin, F. O'Flaherty, *J. Chem. Educ.* **1929**, *6*, 1019–1034.
[12] B. Sengupta, P. K. Sengupta, *Biopolymers* **2003**, *72*, 427–434.
[13] C. Dufour, O. Dangles, *Biochim. Biophys. Acta.* **2005**, *1721*, 164–173.
[14] A. Papadopoulou, R. J. Green, R. A. Frazier, *J. Agric. Food Chem.* **2005**, *53*, 158–163.
[15] M. R. Links, J. Taylor, M. C. Kruger, J. R. N. Taylor, *J. Funct. Foods* **2015**, *12*, 55–63.
[16] V. de Freitas, E. Carvalho, N. Mateus, *Food Chem.* **2003**, *81*, 503–509.
[17] M. Lataza Rovaletti, E. Benítez, N. Martinez Amezaga, N. M. Peruchena, G. L. Sosa, J. Lozano, *Food Res. Int.* **2014**, *62*, 779–785.
[18] M. Mozzicafreddo, M. Cuccioloni, V. Cecarini, A. M. Eleuteri, M. Angeletti, *J. Chem. Inf. Model.* **2009**, *49*, 401–409.
[19] N. F. Brás, R. Gonçalves, N. Mateus, P. a Fernandes, M. J. Ramos, V. de Freitas, *J. Agric. Food Chem.* **2010**, *58*, 10668–10676.
[20] X. Wu, W. He, L. Yao, H. Zhang, Z. Liu, W. Wang, Y. Ye, J. Cao, J. *Agric. Food Chem.* **2013**, *61*, 8829–8835.

[21] B. G. Green, *Acta Psychol.* **1993**, *84*, 119–125.
[22] E. Haslam, M. P. Williamson, N. J. Baxter, A. J. Charlton in *Recent Advances in Phytochemistry, Vol. 33: Phytochemicals in Human Health Protection, Nutrition, and Plant Defense* (Eds.: J. T. Romeo), Springer, New York, **1999**, pp. 289–318.
[23] E. Jöbstl, J. O'Connell, J. P. a Fairclough, M. P. Williamson, *Biomacromolecules* **2004**, *5*, 942–949.
[24] N. J. Baxter, T. H. Lilley, E. Haslam, M. P. Williamson, *Biochemistry* **1997**, *2960*, 5566–5577.
[25] C. Simon, K. Barathieu, M. Laguerre, J. Schmitter, E. Fouquet, I. Pianet, E. J. Dufourc, *Biochemistry* **2003**, *42*, 10385–10395.
[26] A. J. Charlton, E. Haslam, M. P. Williamson, *J. Am. Chem. Soc.* **2002**, *124*, 9899–9905.
[27] F. Canon, R. Ballivian, F. Chirot, R. Antoine, P. Sarni-manchado, J. Lemoine, P. Dugourd, *J. Am. Chem. Soc.* **2011**, *133*, 7847–7852.
[28] R. Ferrer-Gallego, N. Quijada-Morín, N. F. Brás, P. Gomes, V. de Freitas, J. C. Rivas-Gonzalo, M. T. Escribano-Bailón, *Chem. Senses* **2015**, *40*, 381–390.
[29] A. E. Hagerman in *Recent Advances in Polyphenol Research, Vol. 3* (Eds.: V. Cheynier, P. Sarni-Manchado, S. Quideau), Wiley-Blackwell, Oxford, UK, **2012**, pp. 71–97.
[30] R. F. W. Bader, *Atoms in Molecules: A Quantum Theory*, Clarendon Press, Oxford, **1994**.
[31] S. B. Engelsen, C. Monteiro, C. Hervé de Penhoat, S. Pérez, *Biophys. Chem.* **2001**, *93*, 103–127.
[32] J. A. Te, M.-L. Tan, T. Ichiye, *Chem. Phys. Lett.* **2010**, *491*, 218–223.
[33] C. L. Brooks, M. Karplus, B. M. Pettitt, *Proteins: A Theoretical Perspective of Dynamics, Structure and Thermodynamics*, Wiley-Interscience, New York, **1988**.
[34] N. J. M. Amezaga, S. C. Pamies, N. M. Peruchena, G. L. Sosa, *J. Phys. Chem. A* **2010**, *114*, 552–562.
[35] M. J. González Moa, M. Mandado, R. A. Mosquera, *J. Phys. Chem. A* **2007**, *111*, 1998–2001.
[36] R. F. W. Bader, *J. Phys. Chem. A* **1998**, *102*, 7314–7323.
[37] C. Foroutan-Nejad, S. Shahbazian, R. Marek, *Chem. - A Eur. J.* **2014**, *20*, 10140–10152.
[38] T. Karthick, P. Tandon, S. Singh, P. Agarwal, A. Srivastava, *Spectrochim. Acta - Part A Mol. Biomol. Spectrosc.* **2017**, *173*, 390–399.
[39] M. T. Carroll, R. F. W. Bader, *Mol. Phys.* **1988**, *65*, 695–722.
[40] E. Espinosa, E. Molins, C. Lecomte, *Chem. Phys. Lett.* **1998**, *285*, 170–173.
[41] R. D. Tosso, M. Vettorazzi, S. A. Andujar, L. J. Gutierrez, J. C. Garro, E. Angelina, R. Rodríguez, F. D. Suvire, M. Nogueras, J. Cobo, R. D. Enriz, *J. Mol. Struct.* **2017**, *1134*, 464–474.
[42] A. M. Luchi, E. L. Angelina, S. A. Andujar, R. D. Enriz, N. M. Peruchena, *J. Phys. Org. Chem.* **2016**, *29*, 645–655.
[43] P. L. A. Popelier, *J. Phys. Chem. A* **1998**, *102*, 1873–1878.
[44] E. Espinosa, I. Alkorta, J. Elguero, E. Molins, *J. Chem. Phys.* **2002**, *117*, 5529–5542.
[45] C. F. Matta, R. J. Boyd, The Quantum Theory of Atoms in Molecules: From Solid State to DNA and Drug Design, Wiley-VCH, Weinheim, **2007**.
[46] U. Koch, P. L. A. Popelier, *J. Phys. Chem.* **1995**, *99*, 9747–9754.
[47] E. L. Angelina, S. A. Andujar, R. D. Tosso, R. D. Enriz, N. M. Peruchena, *J. Phys. Org. Chem.* **2014**, *27*, 128–134.
[48] L. Estévez, N. Otero, R. A. Mosquera, *J. Phys. Chem.* A **2009**, *113*, 11051–11058.
[49] S. A. Andujar, R. D. Tosso, F. D. Suvire, E. Angelina, N. Peruchena, N. Cabedo, D. Cortes, R. D. Enriz, *J. Chem. Inf. Model.* **2012**, *52*, 99–112.
[50] J. Hernández-Trujillo, C. F. Matta, *Struct. Chem.* **2007**, *18*, 849–857.
[51] K. J. Siebert, P. Y. Lynn, *J. Agric. Food Chem.* **1997**, *45*, 4275–4280.

Submitted: April 5, 2017
Revised: July 3, 2017
Accepted: July 6, 2017

FULL PAPERS

Molecular Dynamic simulations in conjunction with the analysis of the topology of the electron density were used to study protein/polyphenol interactions. The necessary condition for the development of colloidal particles in polyphenol/protein aggregation is the formation of a hydrogen bond that involves a carbonylic oxygen of the protein and an –OH group of the polyphenol. C–H···O interactions play a key role in the stabilization of the aggregate.